International Journal of Mass Spectrometry 386 (2015) 15–23

Contents lists available at ScienceDirect

International Journal of Mass Spectrometry

journal homepage: www.elsevier.com/locate/ijms

# A modified auxiliary excitation signal for achieving unidirectional ion ejection in quadrupole ion trap mass spectrometers operating in the resonance ejection mode

Appala Naidu Kotana [a], Atanu K. Mohanty [a,b,*]

[a] Supercomputer Education and Research Centre, Indian Institute of Science, Bangalore 560012, India
[b] Department of Instrumentation and Applied Physics, Indian Institute of Science, Bangalore 560012, India

ARTICLE INFO

*Article history:*
Received 6 March 2015
Received in revised form 26 May 2015
Accepted 29 May 2015
Available online 9 June 2015

*Keywords:*
Quadrupole ion trap
Resonance ejection
Modified auxiliary dipolar excitation

ABSTRACT

This paper proposes a technique to cause unidirectional ion ejection in a quadrupole ion trap mass spectrometer operated in the resonance ejection mode. In this technique a modified auxiliary dipolar excitation signal is applied to the endcap electrodes. This modified signal is a linear combination of two signals. The first signal is the nominal dipolar excitation signal which is applied across the endcap electrodes and the second signal is the second harmonic of the first signal, the amplitude of the second harmonic being larger than that of the fundamental.

We have investigated the effect of the following parameters on achieving unidirectional ion ejection: primary signal amplitude, ratio of amplitude of second harmonic to that of primary signal amplitude, different operating points, different scan rates, different mass to charge ratios and different damping constants.

In all these simulations unidirectional ejection of destabilized ions has been successfully achieved.



## 1. Introduction

With the purpose of bringing about unidirectional ion ejection in a quadrupole ion trap mass spectrometer (QIT) [1,2], a technique has been proposed in this paper. The QIT has a three electrode geometry mass analyzer consisting of two endcap electrodes and a central ring electrode. The electrodes are shaped so as to produce a linear trapping field within the trap cavity when an oscillatory r.f. potential is applied between the ring and (grounded) endcap electrodes.

In resonance ejection experiments [12–18], a dipolar auxiliary excitation is applied at a fixed frequency, across the endcap electrodes. In these experiments the secular frequency of ions is increased from a value lower than the frequency of the auxiliary excitation, by increasing the amplitude of the r.f. excitation applied between the ring electrode and endcap electrodes. Ion destabilization occurs when the secular frequency of an ion comes into resonance with the fixed frequency of the auxiliary excitation. The resonance ejection mode of operation has advantages over mass selective boundary ejection experiment [13] on account of higher mass range [20,19] and improved resolution [21].

In resonance ejection experiments ions destabilize in the axial direction of the mass analyzer. It is expected that destabilization of ions takes place equally towards the ion source electrode and detector electrode, and consequently only 50 percent of destabilized ions will reach the detector. In this paper we propose a technique that will cause ion ejection, preferentially in one direction, thereby increasing the sensitivity of the mass analyzer.

Our study is based on a simple premise. Consider two signals $y_1$ and $y_2$, given by

$$\begin{aligned} y_1 &= V_1 \cos(2\pi f t + \psi) \\ y_2 &= V_2 \cos(2(2\pi f t + \psi)), \end{aligned} \tag{1}$$

where $y_2$ is a harmonic of $y_1$, $V_1$ is the zero-to-peak amplitude of the signal $y_1$, and $f$ and $\psi$ are frequency and phase of $y_1$ respectively. $V_2$ is the zero-to-peak amplitude of the signal $y_2$. These two signals $y_1$ (–·–) and $y_2$ (---) are plotted in Fig. 1. For making these plots $V_1 = 1$, $V_2 = 1$, $f = 1/2\pi$ and $\psi = 0$ are considered. Also plotted in the figure is the sum of the two signals $y_1$ and $y_2$ (—). As can be seen this sum has clear biased excursion in one direction compared

* Corresponding author at: Supercomputer Education and Research Centre, Indian Institute of Science, Bangalore 560012, India. Tel.: +91 80 2293 3187; fax: +91 80 2360 0135.
*E-mail addresses:* appala@ssl.serc.ernet.in (A.N. Kotana), amohanty@serc.iisc.ernet.in (A.K. Mohanty).

http://dx.doi.org/10.1016/j.ijms.2015.05.011
1387-3806/

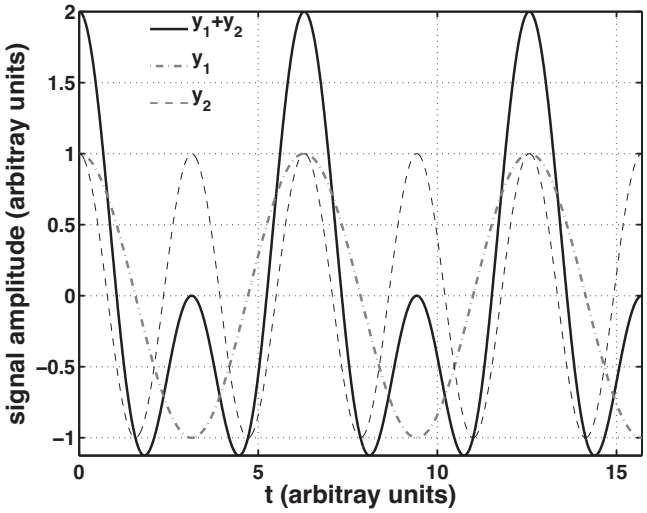


**Fig. 1.** Plot of $y_1$, $y_2$ and $y_1 + y_2$.

to the other, this direction being determined by the sign of $V_2/V_1$. We point out that for the second harmonic to have an impact in bringing about unidirectional ejection of ions, its amplitude ($V_2$) needs to be somewhat large compared to that of the fundamental ($V_1$) because the fundamental is at the resonant frequency and the second harmonic is far removed from it.

The motivation of this study is to see if this summed signal, if applied as the auxiliary excitation in resonance ejection experiments, can lead to a biased ejection of ions in one direction. This is especially important in the context of the scanned mode of operation in which the duration of the time allowed for resonance to occur is limited.

In this paper we propose to apply a modified dipolar signal

$$v_{\text{dipolar}} = V_1\, cos(2\pi ft + \psi) + V_2\, cos(2(2\pi ft + \psi)) \tag{2}$$

consisting of a fundamental component and its second harmonic. The fundamental causes the resonance ejection to occur and second harmonic gives the directionality to ion ejection. This is shown in Fig. 2 which shows the modified dipolar excitation.

We point out that there are earlier experimental studies which have used additional frequencies to improve the sensitivity of ion trap mass analyzers. These include the study of Plomley et al.[5] in which dipolar signal was superimposed on the r.f. to improve sensitivity of QIT, the studies of Gershman et al. [3,4] in which higher harmonics were superimposed on the r.f. to improve the sensitivity of Linear Ion Traps (LIT), and the studies of Wang and Marquette [6,7] in which the r.f. signal was applied across the endcap electrodes to improve sensitivity of QIT. In the last study it was also demonstrated that unidirectional ion ejection was achieved using this scheme.

Our study differs from these in that we have modified the dipolar excitation to include the second harmonic to bring about unidirectional ejection. A notable advantage of our scheme is that low voltages can be used to achieve this biased ejection.

Our simulations are carried out on the truncated QIT. In Section 2 we present the geometry of the QIT taken up for investigation. In Section 3, we present computational methods. Section 4 presents results and discussion. We end by presenting some concluding remarks.

## 2. Geometry considered

The cross-section of the geometry of the QIT is shown in Fig. 2. Also indicated in the figure are the different geometry parameters. In our simulations the electrodes are thin and there are no holes on endcap electrodes.

The radius of the QIT ring electrode is $r_0 = 7$ mm and distance of endcap from centre is $z_0 = 4.9$ mm. The truncation length of the QIT in radial direction is $r_1 = 26.3$ mm and in axial direction is $z_1 = 18.6$ mm.

## 3. Computational methods

We present details of computational methods used in this paper in the following section.

### 3.1. Boundary element method

The boundary element method (BEM) has been used to calculate charge distribution on surfaces of electrodes of ion trap. In this method surfaces of electrodes are divided into small elements and it is assumed that on each of the elements the charge (unknown) is distributed uniformly. The potential on a particular element due to all the elements is expressed in terms of their respective charges, and it has to be the same as the potential applied on the electrode. These expressions will be the system of linear equations with charges on each of the elements as unknown quantities. Once this system of linear equations are solved we get the distribution of charge on the electrodes.

The geometry considered in this paper is axially symmetric, which means that the geometry can be obtained by rotating appropriate curve around a fixed axis. For QIT the curve is a hyperbola and the fixed axis is the $z$-axis. In such geometries the surface of each electrode can be divided into rings. In order to find the charge distribution we follow the method outlined in Tallapragada et al. [22].

Once the charge distribution is computed on each of the ring elements it would be used to find the potential and field at any point due to the ring element. The potential at a given point due to the trap is the sum of potentials due to all ring elements. Similarly, electric field at a given point is the sum of electric fields due to all the ring elements at that point.

The multipole coefficients can also be found using the charge distribution and they are computed using the equations described by Tallapragada et al. [22].

### 3.2. Equations of motion

The equations of motion of an ion is obtained from Newton's second law of motion, which states that the rate of change of momentum is equal to net force acting on it. The net force acting on an ion at a point (say its position vector is $\mathbf{r}$) is the sum of damping force and force due to electric field. The force due to electric field is given by product of charge and electric field at that point. The electric field at $\mathbf{r}$ is the sum of quadrupolar field (field due to trap when endcaps are grounded) and dipolar field (field due to trap when ring is grounded) at $\mathbf{r}$. The equations of motion of the ion in terms of quadrupolar field ($\mathbf{E}^{\text{quad}}$) and dipolar field ($\mathbf{E}^{\text{dip}}$) are given by

$$m\frac{d^2\mathbf{r}}{dt^2} = -c\frac{d\mathbf{r}}{dt} + Q(\mathbf{E}^{\text{quad}} + \mathbf{E}^{\text{dip}}) \tag{3}$$

where $m$ is mass of the ion and $Q$ is charge on the ion. $c = \frac{mm_n}{m+m_n}\frac{p}{k_bT}\frac{Q}{2\varepsilon_0}\sqrt{\alpha\frac{m+m_n}{mm_n}}$ is the damping constant [18], $m_n$ is mass of the bath gas, $p$ is pressure of the bath gas, $k_b$ is Boltzmann constant, $T$ is temperature, $\varepsilon_0$ is permittivity of free space, and $\alpha$ is polarizability of the bath gas.

It is sufficient to look at the $z$-direction equation of motion because the instability of the ion occurs in the $z$-direction. The

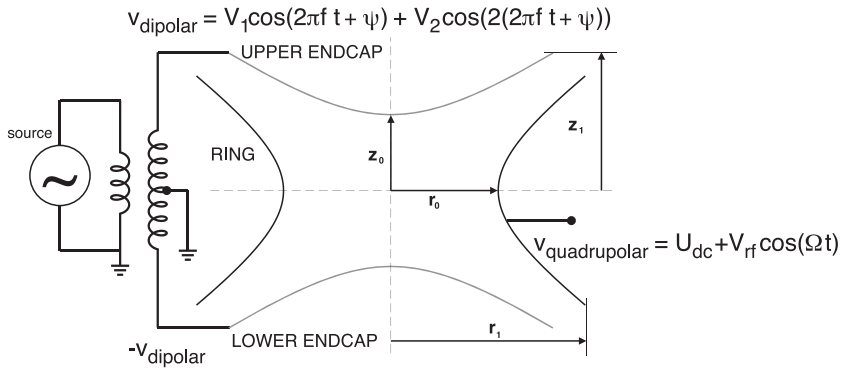


**Fig. 2.** Schematic diagram of resonance ejection experiment with modified auxiliary dipolar excitation signal.

equation of motion in the $z$-direction in terms of respective quadrupolar field component $E_z^{quad}$ and dipolar field component $E_z^{dip}$ is given by

$$m\frac{d^2z}{dt^2} = -c\frac{dz}{dt} + Q(E_z^{quad} + E_z^{dip}) \tag{4}$$

where

$$E_z^{quad} = [U_{dc} + V_{rf}\,cos(\Omega t)]\tilde{E}_z^{quad} \tag{5}$$

and

$$E_z^{dip} = [V_1\ \cos(2\pi ft + \psi) + V_2\,cos(2(2\pi ft + \psi))]\tilde{E}_z^{dip}. \tag{6}$$

In Eq. (5), $U_{dc}$ is DC voltage, $V_{rf}$ is zero-to-peak amplitude of r.f. potential and $\Omega$ is angular frequency of r.f. potential applied between ring electrode and grounded endcap electrodes of the trap. $\tilde{E}_z^{quad}$ is the field along the axis when the ring is at unit potential and endcaps are grounded. Eq. (6) is the expression for $\tilde{E}_z^{dip}$, the field due to auxiliary excitation with an extra harmonic. Here $V_1$, $f$, and $\psi$ are zero-to-peak amplitude, frequency and phase respectively, $V_2$ is amplitude of extra harmonic, and $\tilde{E}_z^{dip}$ is the field along the axis when the ring is grounded and each of the endcaps are kept at unit potential but have opposite polarity. In the conventional resonance ejection experiments, $V_2 = 0$.

The potential along the axis of the trap is calculated using the method followed by Tallapragada et al. [22], and is given by

$$u(z) = \sum_{n=0}^{n=\infty} A_n\left(\frac{z}{L_n}\right)^n, \tag{7}$$

where $A_n$'s are multipole coefficients and $L_n$ is normalizing length.

The $z$-direction field component is obtained by differentiating Eq. (7) with respect to $z$. The field along the axis of the trap in quadrupolar mode of operation, $\tilde{E}_z^{quad}$, is given by

$$\tilde{E}_z^{quad} = \frac{-1}{L_n}\sum_{n=1}^{n=\infty} nA_n^q\left(\frac{z}{L_n}\right)^{n-1} \tag{8}$$

and in dipolar mode of operation $\tilde{E}_z^{dip}$ is given by

$$\tilde{E}_z^{dip} = \frac{-1}{L_n}\sum_{n=1}^{n=\infty} nA_n^d\left(\frac{z}{L_n}\right)^{n-1} \tag{9}$$

where $A_n^q$'s are multipole coefficients obtained by setting unit potential to the ring electrode and endcaps are grounded, and $A_n^d$'s are obtained by keeping the endcaps at unit potential (with opposite polarity) and ring is grounded.

In our computations multipole coefficients up to $A_{10}$ have been considered.

### 3.3. Trajectory calculation

The trajectory of an ion is obtained by solving equations of motion (Eq. (3)). These equations are nonlinear. Since it is difficult to obtain closed form solutions for nonlinear equations, we use a numerical method to compute trajectory. In this paper we use Runge–Kutta fourth order method [23] to find trajectory of the ion.

### 3.4. Computation of ion ejection percentage

The phase, $\psi$ (Eq. (6)), seen by an ion in the trap when the dipolar excitation is switched on, is in the range zero to $2\pi$. When there are multiple ions in the trap, the phase seen by each of the ion is different. In order to calculate the percentage of ions ejecting in one direction, we consider a single ion but with random initial conditions and different phases ($\psi$). The trajectory of ion is calculated for 100 different phases (each phase is obtained in the range 0 to $2\pi$ in steps of $2\pi/100$), and for each phase 100 random initial conditions (positions and velocities) are considered. Out of these 10,000 (100 phases and 100 random initial conditions) trajectories the fraction of trajectories is computed for which the ions are ejected in one direction. We consider 100 times this fraction as the percentage of ions ejected in that direction.

### 3.5. Frequency response curve

The frequency response curve is a curve obtained by plotting the secular frequency on the $x$-axis and amplitude on the $y$-axis. In the curves presented in this paper the secular frequency of the ion has been replaced with the mass of the ion for ease of visualization.

The frequency response curve is determined by fixing r.f. amplitude ($V_{rf}$) and dipolar excitation frequency at a fixed frequency, and mass is varied. The amplitude of a particular mass is taken as the maximum value in the $z$-direction amplitude during ten milliseconds duration. In case the maximum value is beyond the dimension of the trap, amplitude is truncated at $z_0$.

## 4. Results and discussions

It was seen in Section 1 that when two signals were added the resultant signal had a large excursion in one direction compared to the other. In this section we will demonstrate first that by applying a sum of two signals as the dipolar excitation signal in resonance ejection experiments we can indeed cause ejection of ions in a specific direction. Further we will go on to seek optimal values of parameters $V_1$, $V_2$, $V_2/V_1$, and scan rate which will maximize the ejection of ions in a chosen direction. In our study we label this direction of the detector electrode as the positive $z$-direction. We will also

**Table 1**
The number of ions reaching detector for the case $V_1 = 2$ V.

| $V_2$ | $V_2/V_1$ | % ions reaching detector |
|---|---|---|
| −4.0 | −2.0 | 0.0 |
| −1.0 | −0.5 | 13.48 |
| 0.0 | 0.0 | 50.0 |
| 1.0 | 0.5 | 86.52 |
| 4.0 | 2.0 | 100.0 |

show that adding a harmonic to the dipolar excitation signal does not result in any deleterious effect on the performance of the mass analyzer. This will be done by a comparative study of the amplitude response curves obtained in the absence and presence of extra harmonic excitation.

In order to perform the above simulations, we solve Eq. (4) to obtain axial motion of the ion. The trap we considered for these simulations is a truncated quadrupole ion trap (Section 2) that has ring electrode of radius 7 mm. DC voltage ($U_{dc}$) is set to zero, radial r.f. frequency ($\Omega$) is taken as $6.26 \times 10^6$ rad s$^{-1}$, and mass ($m$) of the ion is taken as 78Th. The initial positions are generated randomly such that they are distributed uniformly between $-z_0/5$ and $z_0/5$. Initial velocities are generated randomly using the Maxwell–Boltzmann distribution [10].

The damping constant is calculated assuming helium as the bath gas at pressure 0.1 Pa and the temperature is fixed at 493 K. These conditions remain same throughout these computations unless specified otherwise.

### 4.1. Unidirectional ejection of ions

In order to confirm the preferential ion ejection in the QIT, auxiliary excitation with $V_1 = 2$ V is applied across endcap electrodes at operating point $q_z = 0.66$ ($q_z$ is Mathieu parameter [14]). This simulation has been performed with scan rate 180 μs/Th. The results are shown in Table 1. It can be seen that in the absence of second harmonic ($V_2 = 0$), there is 50 percent of ion ejection in one direction, which is the case in conventional resonance ejection experiments. The introduction of second harmonic with $V_2 = 1$ V results in 86.52 percent ion ejection in one direction, and with $V_2 = -1$ V, it is 13.48 percent ion ejection in that direction. There is 100 percent ion ejection with $V_2 = 4$ V and none of the ions ejecting with $V_2 = -4$ V.

It is evident from these simulations that the additional harmonic in the auxiliary excitation leads to 100 percent ion ejection in one direction, the direction being determined by the sign of the ratio $V_2/V_1$.

### 4.2. Dependence of unidirectional ion ejection on $V_1$

Having seen that it is possible to get unidirectional ejection of ions for $V_1 = 2$ V, we next investigate the dependence of ion ejection on the magnitude of the auxiliary excitation voltage $V_1$. For that we considered $V_1 = 4$ V. This simulation is also carried out at operating point $q_z = 0.66$ with scan rate 180 μs/Th with the same conditions as in Section 4.1. The results are presented in Table 2. It can be seen from the data that for $V_2 = 1$ V, that is for $V_2/V_1 = 0.25$, the percentage of ions ejecting in one direction is 80.54 percent. Conversely, this reduces to 19.46 percent when $V_2/V_1 = -0.25$.

**Table 2**
The number of ions reaching detector for the case $V_1 = 4$ V.

| $V_2$ | $V_2/V_1$ | % ions reaching detector |
|---|---|---|
| −4.0 | −1.0 | 1.1 |
| −1.0 | −0.25 | 19.46 |
| 0.0 | 0.0 | 50.0 |
| 1.0 | 0.25 | 80.54 |
| 4.0 | 1.0 | 98.9 |

It is evident from Tables 1 and 2 that it is possible to achieve unidirectional ejection of ions for both the cases, $V_1 = 2$ V and $V_1 = 4$ V. However, the ratio of $V_2/V_1$ for which this occurs is different for $V_1 = 2$ V and $V_1 = 4$ V.

### 4.3. Dependence of unidirectional ion ejection on the ratio $V_2/V_1$

In order to get a more comprehensive picture of the behaviour of percentage of ions ejecting in one direction with the ratio $V_2/V_1$, we plotted the ratio $V_2/V_1$ on the $x$-axis and percentage of ions ejected in one direction on the $y$-axis. The plots obtained for $V_1 = 2$ V and $V_1 = 4$ V are shown in Fig. 3. These plots are obtained at operating point $q_z = 0.66$ and scan rate 180 μs/Th. These studies have been carried out for $V_2/V_1$ values well beyond the values at which unidirectional ion ejection occurs. This is been done to understand what happens when the amplitude of the harmonic, $V_2$, is considerably larger than the amplitude of the fundamental, $V_1$.

The plot shown in Fig. 3(a) corresponds to $V_1 = 2$ V for the ratio $V_2/V_1$ in the range 0 to ±6. It can be seen from this figure that the percentage of ions ejected in one direction increases to 100 percent when the ratio increase to 1 and remains constant till the ratio reaches close to 4. After this the ions ejecting in that direction decreases. As expected, this picture is reversed in the negative $z$-direction as can be seen from the plot on the negative values of $V_2/V_1$.

The plot shown in Fig. 3(b) corresponds to $V_1 = 4$ V for the ratio $V_2/V_1$ in the range 0 to ±4. It can be seen from this figure that the percentage of ions ejected in one direction increases to 100 percent when the ratio increases to 1, and a further increase in the ratio $V_2/V_1$ causes it to decrease the ejected ion percentage in that direction. Finally around $V_2/V_1 = 4.0$ it reaches 50 percent.

For both the cases $V_1 = 2$ V and $V_1 = 4$ V, it can be seen that the percentage of ions ejecting in one direction increases with respect to the ratio $V_2/V_1$. Finally, when the ratio $V_2/V_1$ is around one, the percentage of ions ejecting in that direction is maximum. Another thing to be noted is that for the case $V_1 = 2$ V, 100 percent ion ejection remains constant over greater range of the ratio $V_2/V_1$. But for the case $V_1 = 4$ V the range of the ratio $V_2/V_1$ for which 100 percent ion ejection happens is narrower in comparison to the case of $V_1 = 2$ V.

In order to understand why the curves peak for a specific range of $V_2/V_1$, we plot Eq. (1) for two values of $V_2/V_1$ corresponding to $V_2/V_1 = 0.2$ and 5. The plots of $y_1$, $y_2$ and $y_1 + y_2$ are presented in Fig. 4. Fig. 4(a) corresponds to $V_2/V_1 = 0.2$ ($V_1 = 1$ and $V_2 = 0.2$) and Fig. 4(b) corresponds to $V_2/V_1 = 5.0$ ($V_1 = 0.2$ and $V_2 = 1$). Comparing these plots to Fig. 1 gives us some insight into what may be happening. The summed signal in Fig. 4(a) and (b) is seen to have an almost equal excursion in the positive and negative direction. In contrast, for the ratio $V_2/V_1 = 1.0$ ($V_1 = 1$ and $V_2 = 1$) as seen in Fig. 1, there is a clear bias in one direction. Clearly, unidirectional ejection of destabilized ions occurs when the auxiliary excitation has a biased excursion in one direction. This happens only for a limited range of the ratio $V_2/V_1$.

Turning to the question of what happens for $V_2/V_1$ values larger than that required to cause unidirectional ion ejection, an inspection of Fig. 3(a) and (b) provides a clue. When $V_2$ is considerably larger than $V_1$, unidirectionality of the ion ejection is lost and the ion ejection tends towards occurring equally in both the directions.

### 4.4. Frequency response curves

In order to demonstrate that performance of the trap is not affected by the addition of harmonic in the auxiliary excitation frequency, we compare frequency response curves in the presence and absence of extra harmonic.

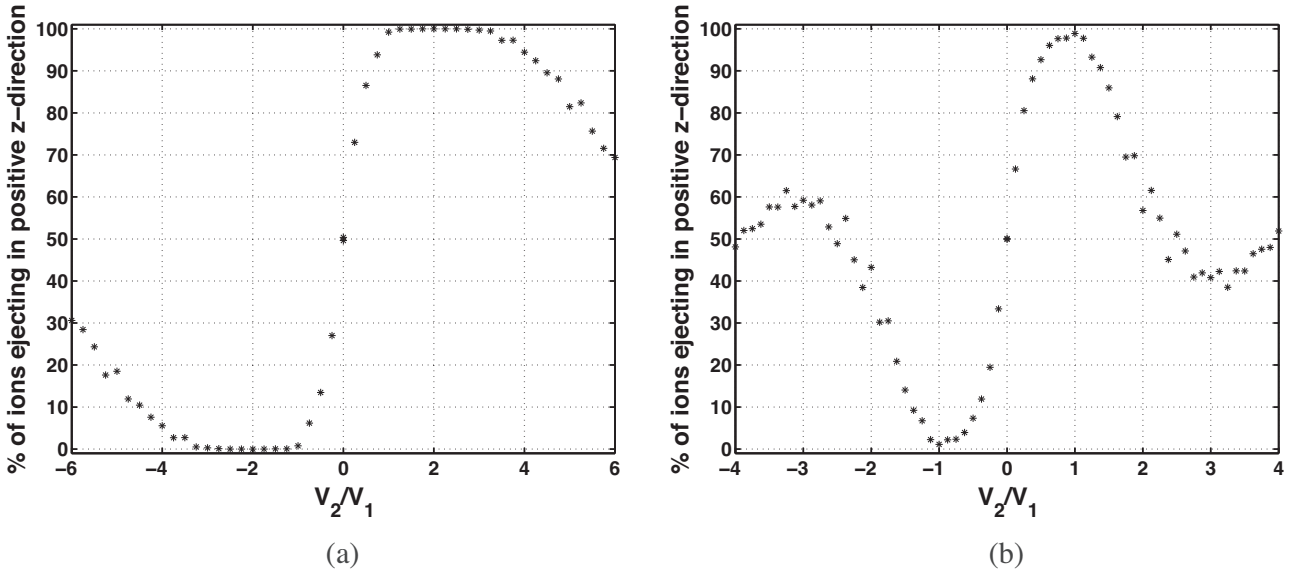


**Fig. 3.** The percentage of ions ejecting in one direction for different $V_1$ with respect to $V_2/V_1$ operated at $q_z = 0.66$ with scan rate 180 μs/Th, (a) $V_1 = 2$ V and (b) $V_1 = 4$ V.

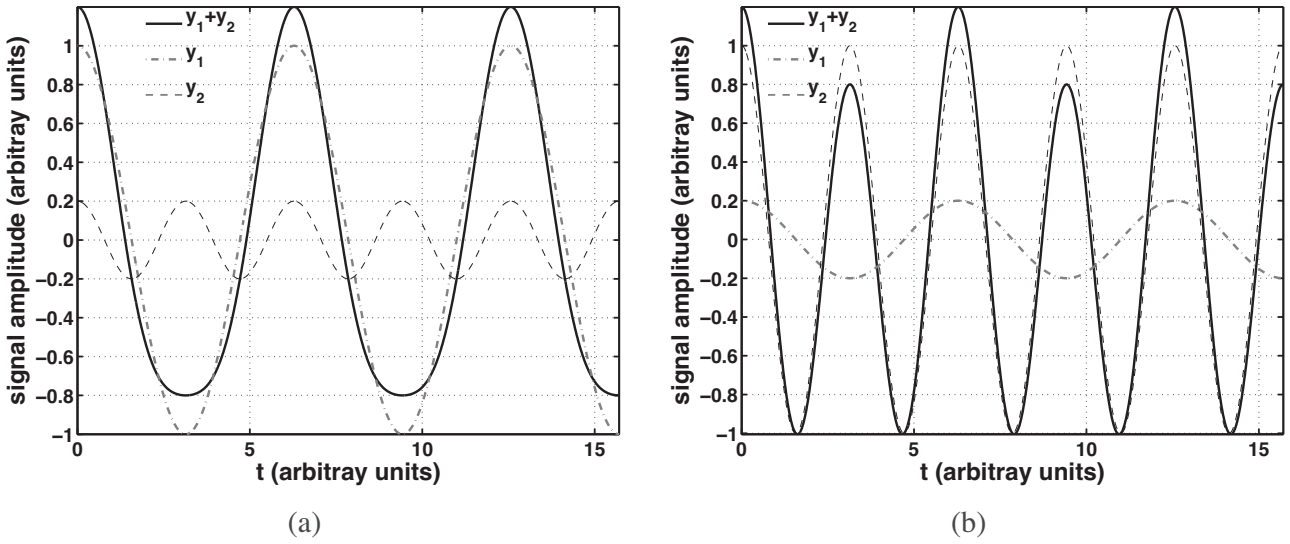


**Fig. 4.** Plots of signals $y_1$, $y_2$ and $y_1 + y_2$ given in Eq. (1): (a) $V_2/V_1 = 0.2$ and (b) $V_2/V_1 = 5.0$.

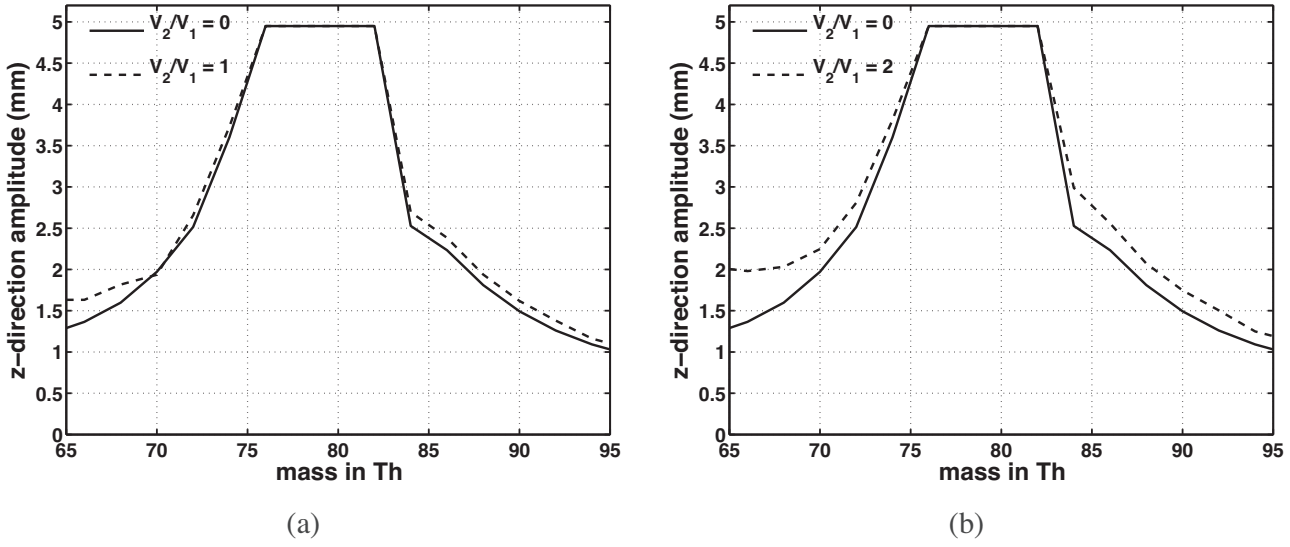


**Fig. 5.** The $z$-direction amplitude in a 7 mm qudrupole ion trap with $V_1 = 2$ V, (a) $V_2 = 2$ V and (b) $V_2 = 4$ V.

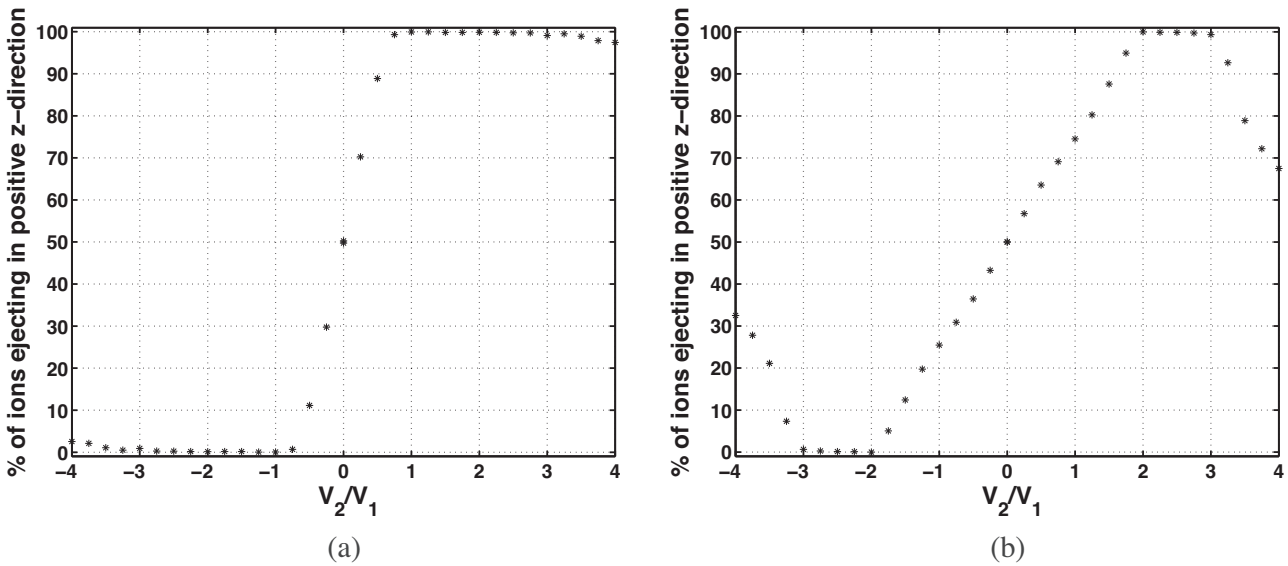


**Fig. 6.** The percentage of ions ejecting in one direction for different $q_z$ with respect to $V_2/V_1$ at $V_1 = 2$ V with scan rate 180 μs/Th, (a) $q_z = 0.72$ and (b) $q_z = 0.78$.

The frequency response curves of the $z$-direction motion are shown in Fig. 5. These are obtained at operating point $q_z = 0.66$ with $V_1 = 2$ V. In these figures mass is shown on the $x$-axis and their respective amplitudes are on the $y$-axis. Fig. 5(a) corresponds to $V_2/V_1 = 1.0$ and Fig. 5(b) corresponds to $V_2/V_1 = 2.0$.

It can be seen from Fig. 5, that the match between curves is better with the ratio $V_2/V_1 = 1.0$ in comparison to the ratio $V_2/V_1 = 2.0$. However, the match is good enough to conclude that the ejection point is unaltered with the introduction of second harmonic. Hence, the sensitivity of the trap can be doubled by introducing second harmonic, without causing any deterioration in its performance.

It should be noted that Fig. 5 does not indicate the resolution of the device. It shows the steady state ion oscillation amplitudes only. A determination of the resolution of the mass analyzer would involve the study of ion motion in the mass scan mode, which is not done here.

### 4.5. Operating point versus $V_2/V_1$

In order to understand the dependence of ratio $V_2/V_1$ on operating point $q_z$, the Mathieu parameter [14], we carried out a study at $q_z = 0.72$, $q_z = 0.78$. The results of the study at $q_z = 0.66$ have already been reported in Fig. 3. It may be pointed out that $q_z = 0.66$ and $q_z = 0.78$ are associated with two well known nonlinear resonances of the trap [11]. The study at $q_z = 0.72$ was to ensure that the specific phenomenon we are observing is not on account of any such non-linear resonance. In this study we considered $V_1 = 2$ V and scan rate 180 μs/Th.

Fig. 6(a) corresponds to $q_z = 0.72$. It can be seen from this figure that the percentage of ions ejecting in one direction increases with respect to the ratio $V_2/V_1$. Finally, there is 100 percent ion ejection in one direction when the ratio $V_2/V_1$ increased to around 1.0, and remains constant in the range around 1–3. Further increase in the ratio causes reduction in ion ejection percent.

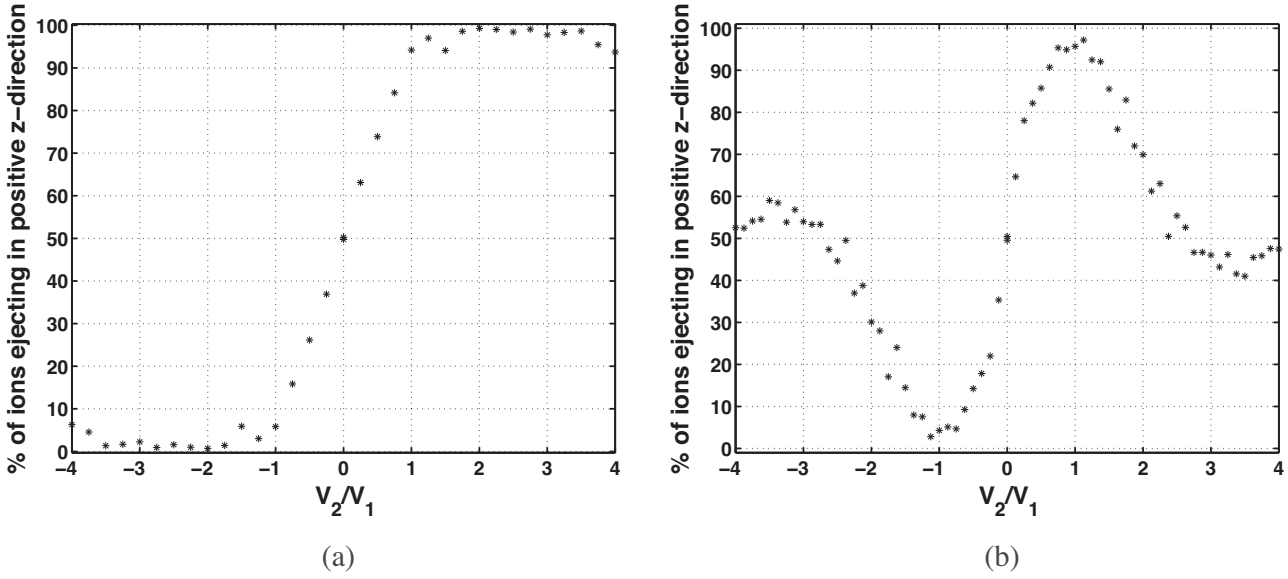


**Fig. 7.** The percentage of ions ejecting in one direction for different $V_1$ with respect to $V_2/V_1$ operated at $q_z = 0.66$ with scan rate 140 μs/Th, (a) $V_1 = 2$ V and (b) $V_1 = 4$ V.

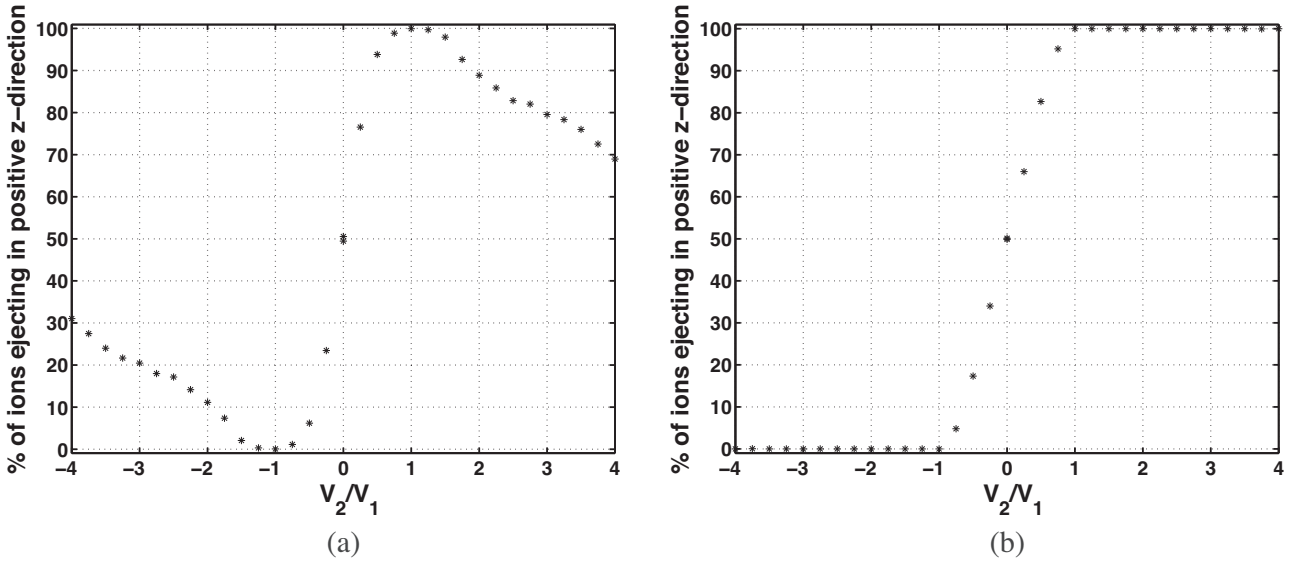


**Fig. 8.** The percentage of ions ejecting in one direction for different mass to charge ratios with respect to $V_2/V_1$ operated at $q_z = 0.72$ with scan rate 180 μs/Th, (a) $m/Q = 40$Th and (b) $m/Q = 100$Th.

Fig. 6(b) corresponds to $q_z = 0.78$. In this case too the ion ejection percentage increases with the ratio $V_2/V_1$ and reaches maximum around $V_2/V_1 = 2.0$, and remains constant in the range around 2–3. This range is smaller in comparison to the case $q_z = 0.72$.

The results of these three studies at $q_z = 0.66$, $q_z = 0.72$, and $q_z = 0.78$ demonstrate that this unidirectional ion ejection is not due to nonlinear resonances since it also occurs at $q_z = 0.72$. However, the ratio of $V_2/V_1$, at which unidirectional ion ejection occurs will be different at the different operating points.

### 4.6. *Scanning rate versus* $V_2/V_1$

Investigations with scan rate of 140 μs/Th are carried out to understand the dependence of $V_2/V_1$ on scan rate, and are compared with our earlier simulations which are carried out at a scan rate 180 μs/Th. This study is carried out at operating point $q_z = 0.66$.

The plots shown in the Fig. 7 are obtained with scan rate 140 μs/Th for $V_1 = 2$ V (shown in Fig. 7(a)) and $V_1 = 4$ V (shown in Fig. 7(b)). It can be seen from these figures that the percentage of ions ejecting in one direction increases with respect to the ratio $V_2/V_1$. Finally, there is 100 percent ion ejection in one direction when the ratio $V_2/V_1$ increased to around 1.

It can be noted from Fig. 7 that the range of $V_2/V_1$ for which 100 percent ion ejection happens is larger for $V_1 = 2$ V in comparison to $V_1 = 4$ V.

The plots shown in the Fig. 3 are obtained with scan rate 180 μs/Th and those in Fig. 7 are obtained with scan rate 140 μs/Th. These figures are similar except there is a little scatter in the plots for the scan rate 140 μs/Th in comparison to scan rate 180 μs/Th.

It is noteworthy that unidirectional ion ejection can be achieved by the introduction of second harmonic for different scan rates too. However the ratio of $V_2/V_1$ at which unidirectional ion ejection will occur may be different for the different scan rates.

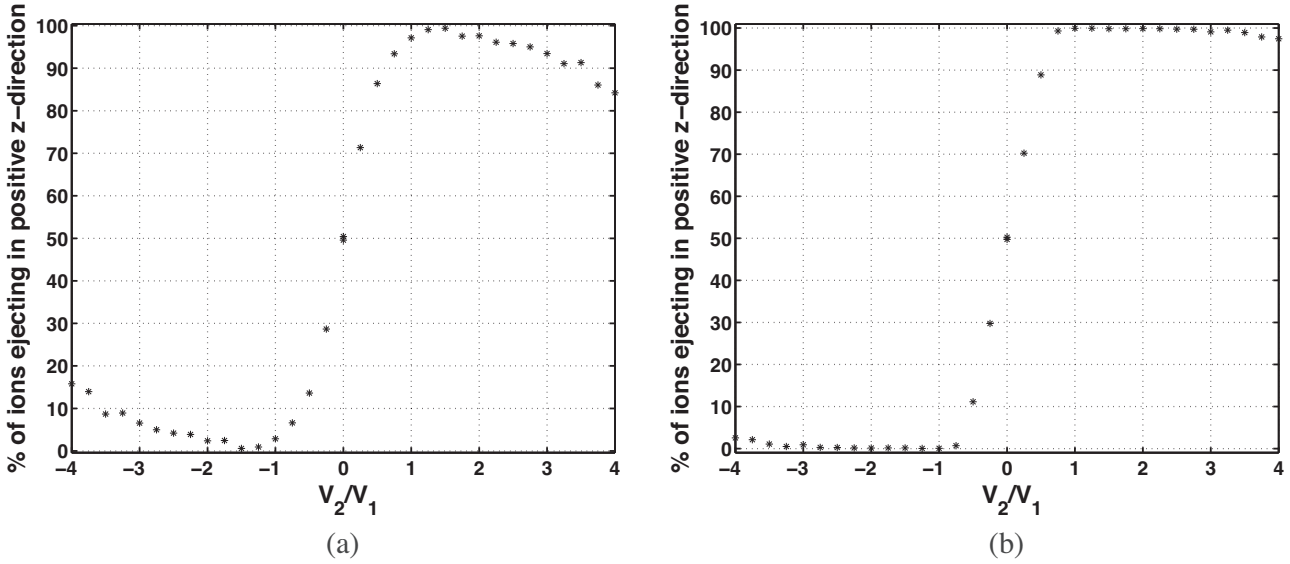


**Fig. 9.** The percentage of ions ejecting in one direction for different pressures with respect to $V_2/V_1$ operated at $q_z = 0.72$ with scan rate 180 μs/Th, (a) $p = 0$ Pa (no damping) and (b) $p = 1.0$ Pa.

### 4.7. Unidirectional ejection for mass to charge ratio 40Th and 100Th

We have carried out simulation with mass to charge ratio 40Th and 100Th to show that unidirectional ion ejection occurs for at mass to charge ratios other than 78Th. This is shown in Fig. 8. For plotting this figure $V_1 = 2$ V, scan rate is of 180 μs/Th, and $q_z = 0.72$. Earlier, unidirectional ejection of ions has already been demonstrated for mass to charge ratio 78Th (Fig. 6(a)).

Fig. 8(a) corresponds to mass to charge ratio 40Th. From this it can be seen that 100 percent of ion ejection occurs around the ratio $V_2/V_1 = 1.0$ and beyond this ratio it starts decreasing with increase of the ratio $V_2/V_1$. Similar observations can be made for mass to charge ratio 100Th, which is shown in Fig. 8(b). Here too 100 ion ejection occurs around $V_2/V_1 = 1.0$, although the range of unidirectional ion ejection is larger for mass to charge ratio 100Th in comparison to mass to charge ratio 40Th.

### 4.8. Damping versus $V_2/V_1$

In order to see the effect of damping on unidirectional ion ejection we have carried out simulations with the bath gas pressure $p = 0$ Pa (no damping) and $p = 1$ Pa. These data are in addition to all our other simulations which have been carried out at $p = 0.1$ Pa. The data related to $p = 0$ Pa and $p = 1$ Pa are shown in Fig. 9. These plots have been generated with $V_1 = 2$ V, scan rate of 180 μs/Th and at $q_z = 0.72$.

Fig. 9(a) corresponds to $p = 0$ Pa, and Fig. 9(b) corresponds to $p = 1$ Pa. In both these plots it can be seen that unidirectional ion ejection occurs close to $V_2/V_1 = 1.0$, with Fig. 9(b) indicating unidirectional ion ejection that occurs for a very wide range $V_2/V_1$ compared to the case when there is no damping.

## 5. Conclusions

This paper proposes a technique for enhancing sensitivity of a quadrupole ion trap mass spectrometer operated in the resonance ejection mode. In this technique a modified auxiliary dipolar excitation signal is applied to the endcap electrodes, the modified signal is a linear combination of the usual dipolar excitation, and its second harmonic.

These simulations have been carried out on a truncated QIT with no apertures on the endcap electrodes. In this sense, this present study has limitations in its scope in view of the fact that earlier studies have shown that the apertures on the endcap electrodes modify the field significantly [8,9].

We have investigated the effect of primary signal amplitude $V_1$, different ratios $V_2/V_1$, different $q_z$ values, different scan rates, different mass to charge ratios and different values of the damping constant, $c$.

It has been shown that for a given amplitude of primary signal, $V_1$ unidirectional ion ejection can be achieved by choosing appropriate amplitude of the second harmonic, $V_2$. The direction of ion ejection is determined by the sign of the ratio $V_2/V_1$.

Finally it is shown that unidirectional ion ejection can be achieved for different $q_z$, scan rates, different mass to charge ratios and different values of the damping constant, $c$. However, the ratio $V_2/V_1$ at which this happens is different for different $q_z$, scan rates, different mass to charge ratios and different values of the damping constant, $c$. In all these simulations it has been seen that for achieving unidirectional ejection the magnitude of $V_2$ needs to be somewhat greater than the magnitude of $V_1$.

The implementation of the technique presented in this paper does not require any modification in the mass analyzer. It requires some modification in the electronics related to the dipolar excitation.

There are several options available for accurately obtaining this modified signal. One possible option would be using a divide-by-two digital counter [24]. A phase locked loop (PLL) [24] with a divide-by-two counter would be another option to synthesize required signal. The waveforms obtained from these techniques may be passed through a band pass filter to obtain sinusoids of required amplitudes. Another possible way of obtaining the required signal is direct digital synthesis (DDS) [25].

Finally, it may be pointed out that the second harmonic does not interfere with the performance of the mass spectrometer, since its frequency falls in the unstable region of the Mathieu plot where no ions are expected to be stable.

## Acknowledgements

We thank Professor A G Menon for discussions during the preparation of this manuscript. We thank the anonymous reviewers for their insightful comments on the manuscript.

## References

[1] W. Paul, Electromagnetic traps for charged and neutral particles, Rev. Mod. Phys. 62 (1990) 531–540.
[2] R.F. Wuerker, H. Shelton, R.V. Langmuir, Electrodynamic containment of charged particles, J. Appl. Phys. 30 (1958) 342–349.
[3] D.J. Gershman, B.P. Block, M. Rubin, M. Benna, P.R. Mahaffy, T.H. Zurbuchen, Higher order parametric excitation modes for spaceborne quadrupole mass spectrometers, Rev. Sci. Instrum. 82 (2011) 125109.
[4] D.J. Gershman, B.P. Block, M. Rubin, M. Benna, P.R. Mahaffy, T.H. Zurbuchen, Comparing the performance of hyperbolic and circular rod quadrupole mass spectrometers with applied higher order auxiliary excitation, Int. J. Mass Spectrom. 319 (2012) 17–24.
[5] J.B. Plomley, C.J. Koester, R.E. March, Determination of N-nitrosodimethylamine in complex environmental matrices by quadrupole ion storage tandem mass spectrometry enhanced by unidirectional ion ejection, Anal. Chem. 66 (1994) 4437–4443.
[6] E.G. Marquette, M. Wang, Proceedings of the 41st ASMS Conference on Mass Spectrometry and Allied Topics, San Francisco, CA, 1993, p. 698a.
[7] M. Wang, E.G. Marquette, U.S. Patent 5,291,017 (1994).
[8] S.T. Quarmby, R.A. Yost, Fundamental studies of ion injection and trapping of electrosprayed ions on a quadrupole ion trap, Int. J. Mass Spectrom. 190 (1999) 81–102.
[9] W.R. Plass, Hongyan Li, R.G. Cooks, Theory, simulation and measurement of chemical mass shifts in RF quadrupole ion traps, Int. J. Mass Spectrom. 228 (2003) 237–267.
[10] D.A. McQuarrie, J.D. Simon, Physical Chemistry: A Molecular Approach, Viva Books, New Delhi, 2011.
[11] G.T. Abraham, A. Chatterjee, A.G. Menon, Escape velocity and resonant ion dynamics in Paul trap mass spectrometers, Int. J. Mass Spectrom. 231 (2004) 1–16.
[12] KaiserJ R.E.Jr., R.G. Cooks, G.C. Stafford Jr., J.E.P. Syka, P.H. Hemberger, Operation of a quadrupole ion trap mass spectrometer to achieve high mass/charge ratios, Int. J. Mass Spectrom. Ion Process. 106 (1991) 79–115.
[13] J.E. Fulford, D. Nhu-Hoa, R.J. Hughes, R.E. March, R.F. Bonner, G.J. Wong, Radio-frequency mass selective excitation and resonant ejection of ions in a three-dimensional quadrupole ion trap, J. Vac. Sci. Technol. 17 (1980) 829–835.
[14] R.E. March, R.J. Hughes, Quadrupole Storage Mass Spectrometry, Wiley-Interscience, New York, 1989.
[15] R.E. March, A.W. McMahon, E.T. Allinson, A.F. Londry, R.L. Alfred, J.F.J. Todd, F. Vedel, Resonance excitation of ions stored in a quadupole ion trap. Part 1. A simulation study, Int. J. Mass Spectrom. Ion Process. 95 (1989) 119–156.
[16] R.E. March, A.W. McMahon, E.T. Allinson, A.F. Londry, R.L. Alfred, J.F.J. Todd, F. Vedel, Resonance excitation of ions stored in a quadupole ion trap. Part 2. Further simulation study, Int. J. Mass Spectrom. Ion Process. 99 (1990) 109–124.
[17] J.D. Williams, K.A. Cox, R.G. Cooks, S.A. McLuckey, K.J. Hart, D.E. Goerlnger, Resonance ejection ion trap mass spectrometry and nonlinear field contributions: the effect of scan direction on mass resolution, Anal. Chem. 66 (1994) 725–729.
[18] N. Rajanbabu, A. Chatterjee, A.G. Menon, Motional coherence during resonance ejection of ions from Paul traps, Int. J. Mass Spectrom. 261 (2007) 159–169.
[19] R.E. Kaiser Jr., J.N. Louris, W. Amy Jonathan, R.G. Cooks, Extending the mass range of the quadrupole ion trap using axial modulation, Rapid Commun. Mass Spectrom. 3 (1989) 225–229.
[20] G.C. Stafford, P.E. Kelley, J.E.P. Syka, W.E. Reynolds, J.F.J. Todd, Recent improvements in and analytical applications of advanced ion trap technology, Int. J. Mass Spectrom. Ion Process. 60 (1984) 85–98.

[21] D.E. Goeringer, W.B. Whitten, J.M. Ramsey, S.A. McLuckey, G.L. Glish, Theory of high-resolution mass spectrometry achieved via resonance ejection in the quadrupole ion trap, Anal. Chem. 64 (1992) 1434–1439.
[22] P.K. Tallapragada, A.K. Mohanty, A. Chatterjee, A.G. Menon, Geometry optimization of axially symmetric ion traps, Int. J. Mass Spectrom. 264 (2007) 38–52.
[23] K. Atkinson, An Introduction to Numerical Analysis, 2nd ed., John Wiley, New York, 1989.
[24] P. Horowitz, W. Hill, The Art of Electronics, 2nd ed., Cambridge University Press, New York, 1989.
[25] J. Vankka, K. Halonen, Direct Digital Synthesizers, Springer, New York, 2001.